

# We are IntechOpen, the world's leading publisher of Open Access books Built by scientists, for scientists

4,800

Open access books available

122,000

International authors and editors

135M

Downloads

Our authors are among the

154

Countries delivered to

TOP 1%

most cited scientists

12.2%

Contributors from top 500 universities



WEB OF SCIENCE™

Selection of our books indexed in the Book Citation Index  
in Web of Science™ Core Collection (BKCI)

Interested in publishing with us?  
Contact [book.department@intechopen.com](mailto:book.department@intechopen.com)

Numbers displayed above are based on latest data collected.  
For more information visit [www.intechopen.com](http://www.intechopen.com)



---

# Dynamic Mathematical Modelling and Advanced Control Strategies for Complex Hydrogenation Process

Roxana Rusu-Both

Additional information is available at the end of the chapter

<http://dx.doi.org/10.5772/65336>

---

## Abstract

Over the last past decades, the number of control system applications in the chemical and petrochemical domains has increased considerably. However, due to the diversity and particularity of chemical processes, there are still many challenges that have to be addressed like: system identification, performance enhancement, monitoring, diagnosis and more importantly closed-loop stability, robustness. Taking into account that most chemical processes are complex, nonlinear MIMO (multi-input multi-output) systems, the challenge is even greater. This book chapter is directed towards the development and the implementation of modern control algorithms for complex and high-risk petrochemical processes, the considered case study being the production of 2 ethyl-hexanol through the 2 ethyl-hexenal hydrogenation process. 2 ethyl-hexanol is mainly used in the production of plasticizers for polyvinyl chloride (PVC) manufacture. In the second part, is described the mathematical modelling of the 2 ethyl-hexenal hydrogenation process including also the simulation and validation of the developed mathematical models. The third part will focus on the design and implementation of conventional control strategy. Section four is dedicated to the design and implementation of several advanced control strategies like Internal Model Control and robust control. The conclusions section represents the last part of the chapter.

**Keywords:** hydrogenation process, mathematical modelling, IMC control, robust control, MIMO control strategy

---

## 1. Introduction

At present time, 2 ethyl-hexanol represents an important raw material in the production of plasticizers, solvents, oils and additives for diesel fuel, making its industrial scale production

---

process of high importance. The industrial scale production of 2 ethyl-hexanol is made either through liquid phase 2 ethyl-hexanal hydrogenation or through gaseous phase 2 ethyl-hexanal hydrogenation. The liquid phase hydrogenation is preferred on industrial scale due to its advantages [1].

The development of complex, accurate mathematical models is an essential step in the dynamic behaviour analysis without expensive experiments and last but not least in the development and testing of control strategies. To this end, for the 2 ethyl-hexanal hydrogenation process was developed at first a distributed parameter mathematical model validated using experimental data. It consists of a system of partial differential equations based on mass (total and component) and energy conservation laws. In order to analyse the dynamic behaviour and to emphasize the interactions between the parts of a hydrogenation process a dynamic study was performed. Several scenarios have been carried out in order to evaluate the dynamic behaviour. The one presented in this chapter is the study of the catalyst deactivation effect. The effect of a variation of the input flow temperature of the streams as well as the effect of a change in the reactor load: the volumetric ratio between the 2 ethyl-hexanal flow rate and the recirculated 2 ethyl-hexanol flow rate are worth to study. The dynamic behaviour study shows the complexity of the hydrogenation process due to heat, mass and kinetic interactions, which are dependent on the operating conditions, reactor loading as well as on the trajectory from one state to another.

Unfortunately, despite their accuracy, detailed, nonlinear mathematical models are too complex for efficient use in controller design so the considered approach is the use of a simple model of the process, which describes its most important properties in combination with an advanced control algorithm which takes into account the model uncertainties, the disturbances and command signal limitations.

To this end, another mathematical model—operational model—is determined based on the main connections between input and output parameters of the process and was obtained based on the result analysis from both simulations step responses related to a distributed parameter model and the experimental data.

For the hydrogenation process presented in this case study, various methods of control were designed: conventional PID control, internal model control (IMC) and robust control in order to find the optimal solution.

The two main control objectives of all the applied control strategies are: (a) to maintain the inlet reactor temperature below an imposed critical value; (b) to ensure a high 2 ethyl-hexanol (product) concentration. From a technological point of view the reactor inlet temperature can be controlled by modifying the 2 ethyl-hexanol recirculated flow rate. The product concentration is influenced by the reactant flow rates and also by the catalyst degree of activity which acts as a variable disturbance. The catalyst degree of activity will continuously decrease as the hydrogenation reaction takes place up to the point it needs to be replaced. However, during this period, this effect can be compensated by continuously increasing the input temperature of the reactants.

For analysis purposes, all proposed control structures were implemented in MATLAB/SIMULINK environment. The simulation scenarios are presented in comparison for all designed control strategies. The two main objectives of the scenarios are the set-point tracking analysis and disturbance rejection analysis. A robustness analysis is also performed.

Finally, by analysing all the advantages and disadvantages of the designed control structures the final solution recommended for the control of the 2 ethyl-hexanal hydrogenation process is the robust control. The concluding remarks are formulated in the last section of the chapter.

## **2. Mathematical models of the 2 ethyl-hexanal hydrogenation process: simulation and validation**

The mathematical modelling of an industrial scale process is a complex problem requiring the following steps: (a) Choosing the model structure based on physical knowledge; (b) Determining and estimating the model parameters from the available data; and (c) Accuracy evaluation of the developed model (model validation) based on experimental data.

The model validation step is closely related to the parameter estimation step. As a result of the estimation procedure it must be examined to what extent the model really explains the real plant behaviour. This aspect can be highlighted by exciting the system model with the same input signal and studying the nature and value of the difference between the model output signals and the real plant variables.

### **2.1. Nonlinear mathematical model**

Based on laws of mass conservation and energy conservation, the mathematical model determined in this section for the hydrogenation process 2 ethyl-hexanal is nonlinear. A dynamic mathematical model can be used to simulate complex mass transfer phenomena and to understand processes occurring inside the reactor. So far there are various models proposed in the literature [2, 3] for the hydrogenation reaction kinetics, but there is no mathematical model to describe the processes taking place inside the hydrogenation reactor. There is a need to develop equations, to determine the parameters and boundary conditions that form the mathematical model consisting of differential equations with partial derivatives. The spatially distributed nature of the process is generally unnoticed or ignored and the control techniques are applied using conventional approximate models with concentrated parameters, identified by experiments input/output. Because these simple models ignore the spatial nature of the process, they often suffer from the close interaction and apparent delays due to diffusion and convection phenomena inherent in such processes. Hence, the need for a modelling procedure that generates a general model, a model that takes into account the spatial structure of the process variable and is deduced from the input and output measured data.

The production of 2 ethyl-hexanol through the liquid phase 2 ethyl-hexenal hydrogenation is depicted in **Figure 1**.

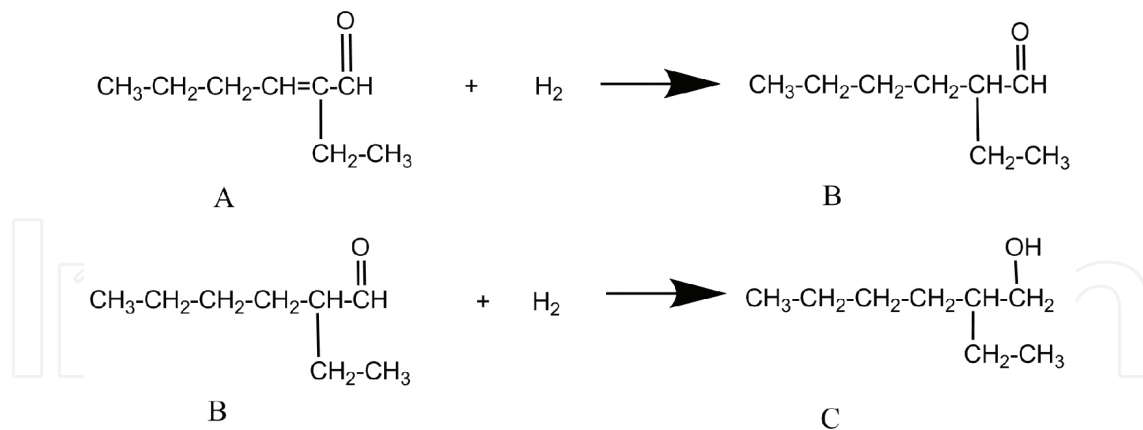


**Figure 1.** Hydrogenation reaction: A—2 ethyl-hexenal, B—2 ethyl-hexanal, C—2 ethyl-hexanol.

As it can be observed, the production of 2-ethyl hexanol is in fact two successive hydrogenation reactions. Thus, the reaction product of the first hydrogenation reaction—2-ethyl-hexanal—is a reactant in the next one. In the hydrogenation process n-butanol and iso-butanol can be obtained as side products of some side reactions. Also, symmetric or asymmetric C8 ethers can be obtained through the etherification reaction of butanols. These side reactions are favoured by operating parameters like: input flows through the reactor, inlet temperature. However, for mathematical modelling purposes only the main reaction will be considered and the following assumptions are made: the model parameters are considered to be constant on the radial section of the reactor; both liquid and gas velocity are considered constant; adiabatic reactor; perfect mixing is considered and the chemical reactions occur only at the catalyst surface. Also, in the reaction zone the following phenomena occur: mass transfer through the volume element  $dz$  (theoretical plate); 2 ethyl-hexanal hydrogenation on the catalyst surface and heat transfer through volume element  $dz$ .

The component mass transfer is essential in a heterogeneous reactor with several phases (gas, liquid) because the reactants have to pass from one phase to another making the modelling of gas-liquid-solid mass transfer process a crucial step. Substances from a gas phase (hydrogen) and a liquid (2 ethyl-hexenal) are transformed on the surface of a solid catalyst (nickel on silica). One of the most important factors in the chemical reaction is the reaction rate (reaction kinetics). In the present case there are two rates of reaction:  $r_1$ , which relates to the hydrogenation of 2 ethyl-hexenal and  $r_2$ , which relates to the hydrogenation of 2 ethyl-hexanal (intermediate product). For this particular case the chosen catalyst is nickel (Ni) based catalyst on a silica (Si) support. Considering the literature studies [2] for the Ni catalyst supported on Si, the best model to express the reaction rate of the proposed model is:

$$r_1 = \frac{k_1 \cdot K_{enal} \cdot K_H \cdot C_{enal} \cdot C_{H_2}}{(1 + K_{enal} \cdot C_{enal} + K_{anal} \cdot C_{anal} + \sqrt{K_H \cdot C_{H_2}})^3} \quad (1)$$

$$r_2 = \frac{k_1 \cdot K_{anal} \cdot K_H \cdot C_{anal} \cdot C_{H_2}}{(1 + K_{enal} \cdot C_{enal} + K_{anal} \cdot C_{anal} + \sqrt{K_H \cdot C_{H_2}})^3} \quad (2)$$

where enal is 2 ethyl-hexanal, anal is 2 ethyl-hexanal, oct is 2 ethyl-hexanol, H is hydrogen,  $K_i$  ( $\text{m}^3/\text{mol}$ ) is the adsorption equilibrium constant for the component  $i$  ( $i$ : enal, anal, H),  $k_i$  ( $\text{m}^3/\text{s kg}$ ) is rate constant of the surface reaction  $i$ , ( $i$ :1,2),  $C_i$  ( $\text{kmol}/\text{m}^3$ ) concentration of component  $i$ .

In industrial scale heterogeneous reactors, the catalyst ages gradually and gets deactivated to the point it becomes inefficient and needs to be replaced. The dependence between the catalyst activity degree and the reaction rate can be expressed as follows:

$$r_i = r_i \cdot e^{-k_D t} \quad (3)$$

where  $k_D$  is the catalyst degree of deactivation.

The reaction rates expression should also include the temperature dependence of the reaction rate constants and absorption constants, which must comply with the Arrhenius law [4] given by:

$$k_i = k_0^i \cdot e^{-\frac{E}{RT}} \quad (4)$$

where  $E$  is the activation energy and  $T$  is the temperature.

The developed total and component mass balance equations are as follows:

$$\begin{cases} \frac{\partial Q_L}{\partial t} = -v_L \frac{\partial Q_L}{\partial z} + v_G \cdot S \cdot M_{H_2} \cdot a_v \cdot N_{H_G} \\ \frac{\partial Q_G}{\partial t} = -v_G \frac{\partial Q_G}{\partial z} - v_G \cdot S \cdot M_{H_2} \cdot a_v \cdot N_{H_G} \end{cases} \quad (5)$$

$$\begin{cases} \frac{\partial C_H^L}{\partial t} = -v_L \frac{\partial C_H^L}{\partial z} + a_v \cdot N_{H_G} - vph \\ \frac{\partial C_H^G}{\partial t} = -v_L \frac{\partial C_H^G}{\partial z} - a_v \cdot N_{H_G} \\ \frac{\partial C_{enal}}{\partial t} = -v_L \frac{\partial C_{enal}}{\partial z} - r_1 \cdot \rho_{sol} \\ \frac{\partial C_{anal}}{\partial t} = -v_L \frac{\partial C_{anal}}{\partial z} + (r_1 - r_2) \cdot \rho_{sol} \\ \frac{\partial C_{oct}}{\partial t} = -v_L \frac{\partial C_{oct}}{\partial z} + r_2 \cdot \rho_{sol} \end{cases} \quad (6)$$

and the heat balance equations for the liquid and gas phases are

$$\begin{cases} \frac{\partial T_L}{\partial t} = -v_L \frac{\partial T_L}{\partial z} - \sum \frac{\Delta_R H_i \cdot r_i}{c_{pL}} \\ \frac{\partial T_G}{\partial t} = -v_G \frac{\partial T_G}{\partial z} - \sum \frac{\Delta_R H_i \cdot r_i}{c_{pG}} \end{cases} \quad (7)$$

All the parameters are detailed in the nomenclature section.

An important feature of the three-phase reactors is the hydrodynamic characteristic. One of the hydrodynamics parameters with high influence on the performance of the three-phase

reactor is the pressure loss of the two-phase mixture. The pressure loss in the functional layer is an important parameter, which depends on the amount of energy required to operate and which also correlates the interphase mass transfer coefficients. The friction pressure loss can be calculated using equation ERGUN [5]:

$$\delta = \frac{1-\varepsilon}{\varepsilon^3} \left( 1.75 + 150 \frac{1-\varepsilon}{Re_p} \right) \frac{\rho v^2}{d_p} \quad (8)$$

where  $\varepsilon$  is layer void fraction, and  $v$ ,  $\nu$ ,  $\rho$  are considered for the phase for which the pressure loss is computed.

The dynamic process simulator was implemented in MATLAB programming environment along with graphical extension to SIMULINK. The process simulator, being represented by a mathematical model comprising a system of nonlinear partial differential equations, was implemented as a function-s: S-function.

To solve the partial differential equations the finite difference method [6] was used. According to this method, the derivatives were written as finite differences. The solution domain must be covered with a network of nodes in order to apply the proposed method. Theoretically, the approximation of the exact solution will be better if the number of nodes included in the network is greater. To approximate the concentrations, temperature and pressure over time and space (height of the reactor) 100 discretization points (the number of theoretical plates) were chosen, being considered the best choice between the complexity of the model and the accuracy of the results. This method is reasonably simple, robust and is a good general candidate for the numerical solution of differential equations.

## 2.2. Validation and dynamic behaviour analysis of the nonlinear mathematical model

The developed nonlinear, distributed parameter mathematical model was calibrated and tested based on experimental data acquired from a functional 2 ethyl-hexanal hydrogenation reactor at Oltchim S.A. company, Romania.

The calibration process was performed taking into account the constructive characteristics of the hydrogenation reactor. The height of the reactor is approximately 20 m, with a diameter of 1 m, while the height of the catalyst is around 18 m. The reactants (hydrogen – gaseous phase – and 2 ethyl-hexanal – liquid phase) are fed at the top of the reactor. Perfect mixing can be considered because the reactor is equipped with a fine sifter at the top. The product (2 ethyl-hexanol) is extracted at the bottom of the reactor. Part of the product is cooled to 90–100 °C in a heat exchanger and recirculated at the top to maintain the inlet temperature below 160 °C. The operating temperature of the reactants is around 100 °C. The plant is also equipped with a heater, to be able to increase the input temperature of the reactants as the catalyst gets deactivated. The flow ratio between the 2 ethyl-hexanal flow and the recirculated 2 ethyl-hexanol flow must be maintained at a specific value in order to maintain the output temperature below the critical value. The main reactor operating point is characterized by the following parameter values: hydrogen flow of 1250 – 1300 (m<sup>3</sup>/h), 2 ethyl-hexanal flow of 4 (m<sup>3</sup>/h), recirculated 2 ethyl-hexanol flow of 24 – 32 (m<sup>3</sup>/h).

The accuracy of the developed mathematical model was tested in different operating points and the comparison between the simulated results and the experimental data in the main operating point is presented in **Table 1**.

Parameter	Simulated value	Plant data
Hydrogen concentration (Kmol/m <sup>3</sup> )	0.078	0.0549
2 ethyl-hexanal concentration (Kmol/m <sup>3</sup> )	0.0021	0.0020
2 ethyl-hexanol concentration (Kmol/m <sup>3</sup> )	5.346	5.32
Output temperature (K)	441.6	441.3

**Table 1.** Mathematical model validation.

The standard deviation is between 5 and 10 % in all cases. This indicates the presence of an acceptable systematic error. The evolution of the main parameters can also be observed in **Figures 2–4**.

By choosing 100 discretization points the height of the theoretical plates of the reactor is 0.2m. Taking into account the diameter of the reactor (~1m) it can be considered that the concentration of 2 ethyl-hexanol and the temperature of the product are constant along the theoretical plate. However, to prove this assumption, a study was performed on the influence of the number of discretization points on the accuracy of the results. The simulation results are presented in the **Figures 5 and 6**, considering 80, 100 and 125 discretization points. As can be observed from the figures, there are no significant changes in the accuracy of the model, the differences being only at the second decimal.

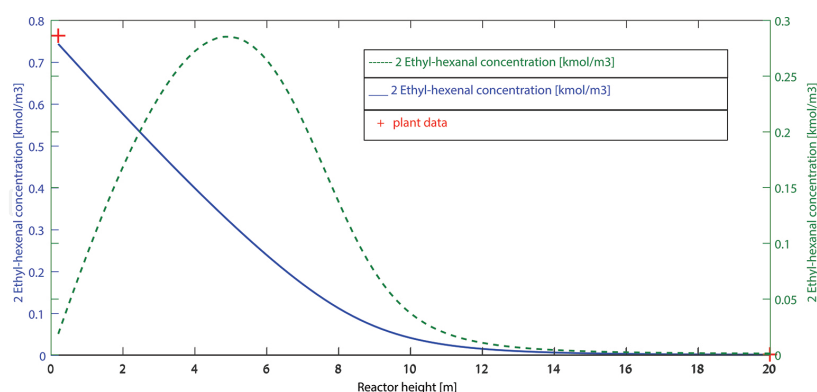


**Figure 2.** 2 ethyl-hexanal and 2 ethyl-hexanal concentration evolution: simulated vs. plant data.

Another important study that needs to be performed to prove that the developed mathematical model captured the hydrogenation mechanism is a dynamic behaviour study. To this end, it is necessary to evaluate that the model captures the effect of catalyst deactivation [7]. By analysing the experimental data it was concluded that the catalyst degree of activity decreases up to 50% after 4 months of continuous functioning. **Figure 7** presents the effect of catalyst



deactivation on the product concentration by maintaining the reactants input flow and temperature constant.

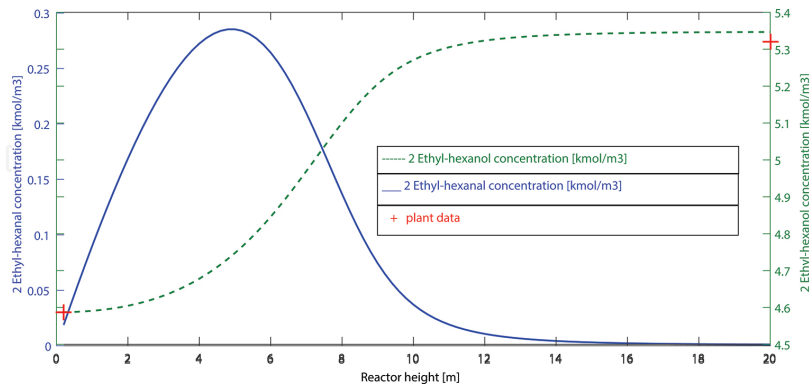


Figure 3. 2 ethyl-hexanal and 2 ethyl-hexanol concentration evolutions: simulated vs. plant data.

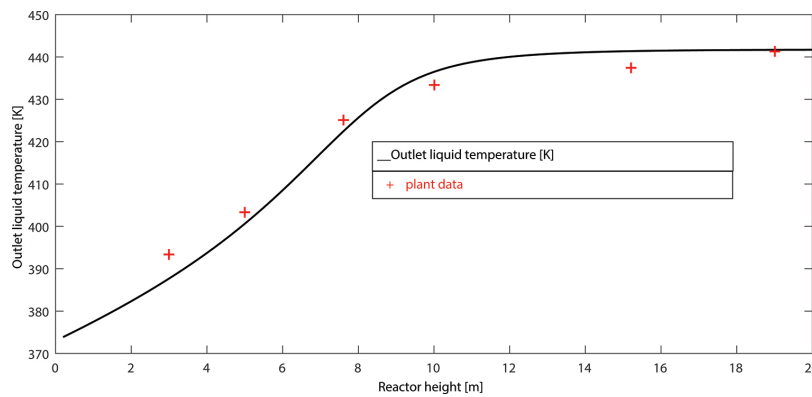


Figure 4. Product temperature evolution: simulated vs. plant data.

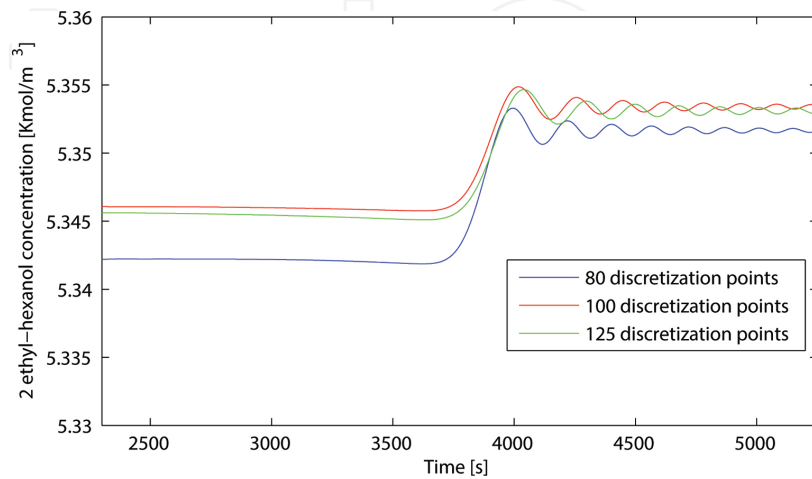


Figure 5. 2 ethyl-hexanol concentration evolution: 80, 100 and 125 discretization points.

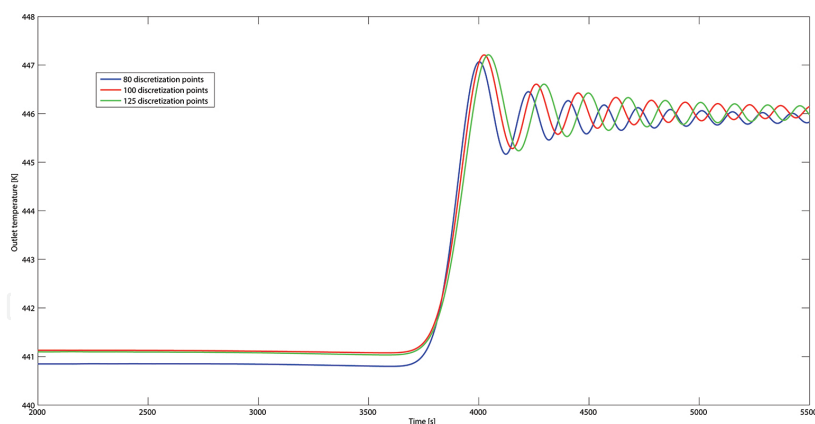


Figure 6. Outlet temperature evolution: 80, 100 and 125 discretization points.

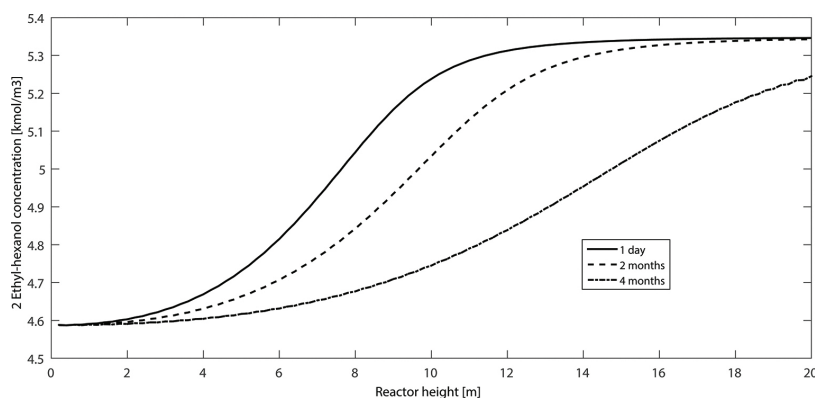


Figure 7. Catalyst deactivation effect on the product concentration.

It is obvious that the catalyst deactivation influences considerably the quality of the product increasing the production costs. This effect can be diminished if the input temperature of the reactants is gradually increased as the catalyst gets older.

### 2.3. Operational mathematical model: development and validation

Based on the previously presented studies, it can be concluded that the hydrogenation process dynamics ethyl 2-hexanal is very complex; thus, it is only normal that the resulting model is nonlinear, higher order with distributed parameters. The only problem is that highly complex models are difficult to use in the development of most control strategies, being more appropriate for control strategy testing. For this reason it is necessary to design a simpler, linear operation model to be used in control design. There are two possible approaches. The first one infers model reduction methods and linearization which can be troublesome. In this section is presented a more unconventional approach, developing a simpler operational model based on the main connections between input and output parameters, using experimental identification methods and the developed nonlinear mathematical model. The results will be validated by simulation.

To this end, by analysing the hydrogenation process and based on the process engineers experimental knowledge the main input variables are considered to be: input flow of 2 ethyl-hexanal, recirculated input flow of 2 ethyl-hexanol, input temperature of the reactants and hydrogen pressure. The main output variables are considered to be the 2 ethyl-hexanol concentration and the output temperature which is critical. Nevertheless, the dependence between the input and the output variables is considered to be of second order as follows:

$$\begin{bmatrix} T_{out} \\ C_{out} \end{bmatrix} = \begin{bmatrix} \frac{K1 \cdot e^{-\sigma s}}{T1 \cdot s^2 + T2 \cdot s + 1} & \frac{K2 \cdot e^{-\sigma s}}{T3 \cdot s^2 + T4 \cdot s + 1} \\ \frac{K3 \cdot e^{-\sigma s}}{T5 \cdot s^2 + T6 \cdot s + 1} & \frac{K4 \cdot e^{-\sigma s}}{T7 \cdot s^2 + T8 \cdot s + 1} \end{bmatrix} \begin{bmatrix} Q_{oct} \\ T_{in} \end{bmatrix} + \begin{bmatrix} \frac{K5 \cdot e^{-\sigma s}}{T9 \cdot s^2 + T10 \cdot s + 1} & \frac{K6 \cdot e^{-\sigma s}}{T11 \cdot s^2 + T12 \cdot s + 1} \\ \frac{K7 \cdot e^{-\sigma s}}{T13 \cdot s^2 + T14 \cdot s + 1} & \frac{K8 \cdot e^{-\sigma s}}{T15 \cdot s^2 + T16 \cdot s + 1} \end{bmatrix} \begin{bmatrix} Q_{enal} \\ P \end{bmatrix} \quad (9)$$

The parameter values are determined using experimental identification methods and considering step variations of the recirculated 2 ethyl-hexanol flow ( $Q_{oct}$ ), input temperature of reactants ( $T_{in}$ ). The same step variations are considered for the 2 ethyl-hexanal input flow ( $Q_{enal}$ ) and the hydrogen input pressure ( $P$ ) even if these parameters are considered to be constant in normal mode of operation. For validation **Figure 8** presents the simulated values obtained for the output temperature and considering a step variation in the recirculated 2 ethyl-hexanol flow.

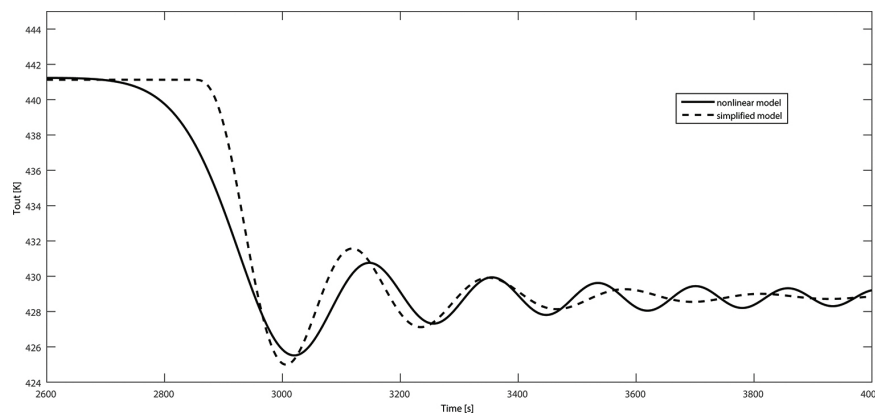


**Figure 8.** Output temperature evolution: operational model vs. nonlinear model.

### 3. Design and implementation of conventional control strategy

Conventional PID controllers are the most common control solution in the industry. Most of the research deals with mono-variable (single input single output—SISO) processes. However, most industrial processes are by their nature multi-variable (multi-input multi-output—MIMO). Using mono-variable controllers for each output variable, even if it is a solution easy to apply, it will lead to inferior performances. It is possible that despite the fact that each individual PID loop control works, the overall PID control structure to fail. For this reason there is a demand for the development of multi-variable PID control strategies to compensate

the effect of functional interactions between variables from many companies that consider the interactions between variables in multi-variable systems as the main common problem in the industry.

The hydrogenation process is characterized by the presence of time delays of approximately 30 minutes. The difference between the dead time of each input-output pair is about 1–2 minutes. For this reason, the dead time is considered to be identical for all input-output pair. A typical approach to deal with time delay is the non-delayed output prediction [8, 9]. The non-delayed output may be estimated and the controller can be computed as for a process without delay. The most popular output predictor is the Smith predictor.

Currently, the 2 ethyl-hexanal hydrogenation plant is operated using the feed forward control (indirect, open-loop control). Thus, using methods sometimes simple, sometimes complicated (even in closed loop), the following parameters are controlled and adjusted to the desired level: the 2 ethyl-hexanal input flow, the recirculated 2 ethyl-hexanol flow, hydrogen input pressure and the reactant input temperature. At present time, an operator decides whether or not to manually modify the control loops set points to maintain the same process parameters and product specifications. To achieve a more effective operation of the hydrogenation process, both conventional and advanced control methods require a closed-loop control structure by including the reaction from the output.

In order to develop a multi-variable PID control, the operational model described in the previous section determined by the Eq. (9) will be used. The desired multi-variable controller matrix has the following form:

$$H_R(s) = \begin{bmatrix} H_{R11}(s) & H_{R12}(s) \\ H_{R21}(s) & H_{R22}(s) \end{bmatrix} \quad (10)$$

where  $H_{R11}$ ,  $H_{R22}$  intended for direct adjustment of output variables and  $H_{R12}$ ,  $H_{R21}$  are intended to counter act the interactions between input and output channels. The four controllers are computed by imposing a phase margin  $\gamma_k = 60^\circ$  [9].

The obtained controllers are described by:

$$\begin{aligned} H_{R11} &= 1.3259 \left( 1 + \frac{1}{102.3018 \cdot s} \right); H_{R12} = 2.733 \left( 1 + \frac{1}{106.667 \cdot s} \right); \\ H_{R21} &= 595.6621 \left( 1 + \frac{1}{90.4977 \cdot s} \right); H_{R22} = 223.8721 \left( 1 + \frac{1}{119.0476 \cdot s} \right) \end{aligned} \quad (11)$$

**Figure 9** presents the closed loop Smith predictor control structure using a PID control.

The next step is to test and evaluate the performances of the developed control strategy by analysing its ability to reject disturbance effects, respectively, the set point tracking capability. In the first scenario, a reference variation of 10 K for the first output value (outlet temperature of the product,  $T_{out}$ ) is considered. The simulation results are presented in **Figure 10**.

The second scenario is designed to test the control system capability to counteract the disturbance effects. Hence, a 6 % step variation in the 2 ethyl-hexanal input flow is considered for the results presented in **Figure 11**.

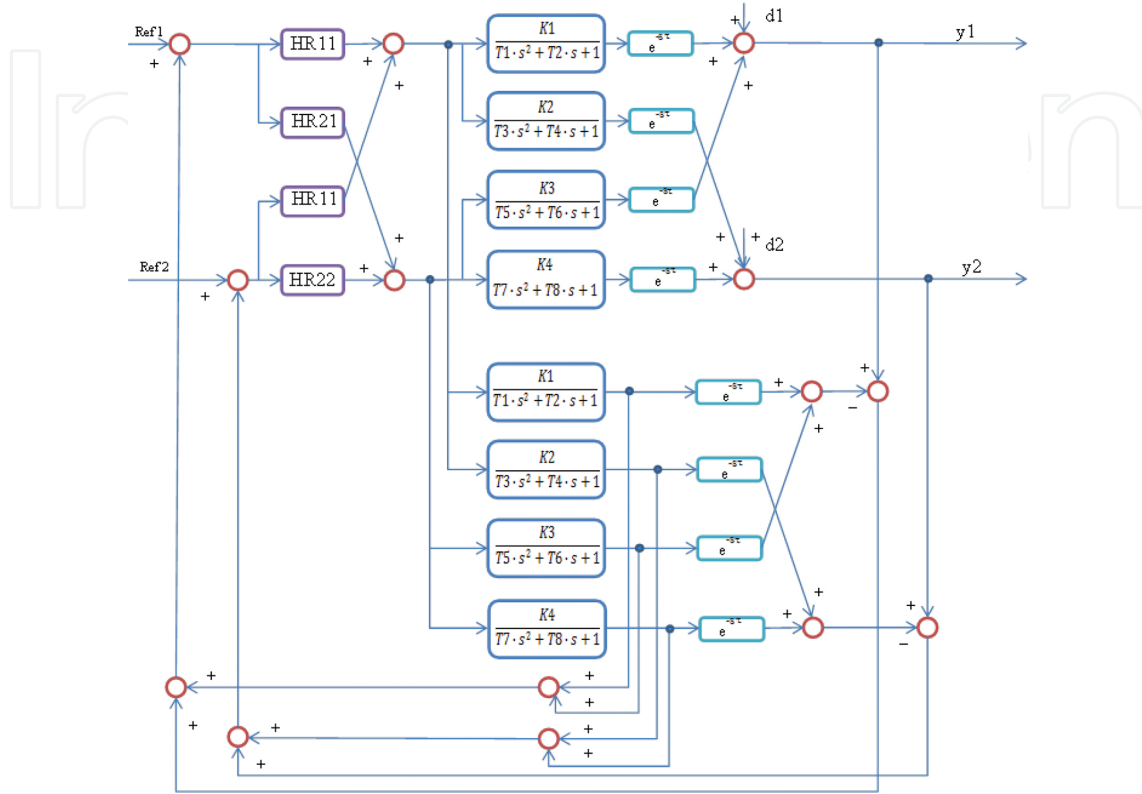


**Figure 9.** Closed loop control structure: conventional PID control in MIMO-SP structure.

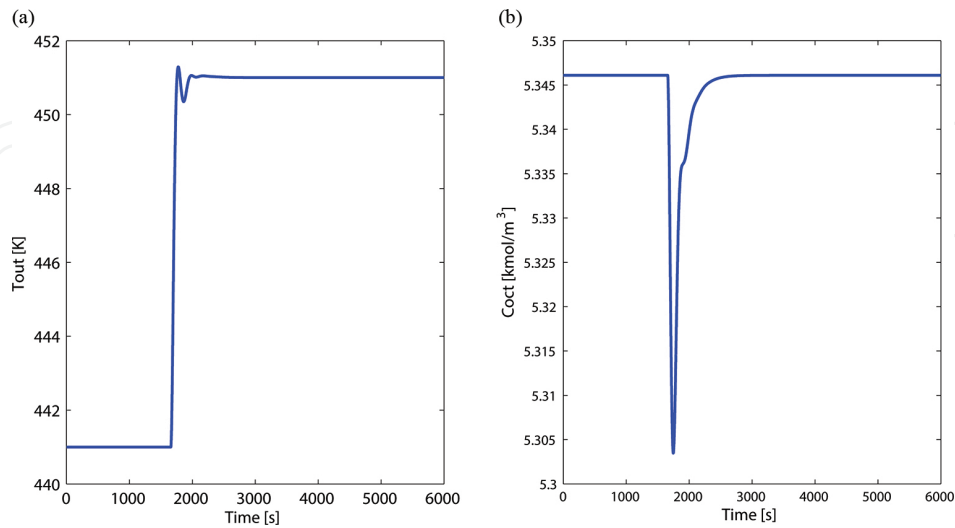


**Figure 10.** Output temperature reference step variation of 10 K: (a) output temperature evolution and (b) 2 ethyl-hexanal concentration evolution.

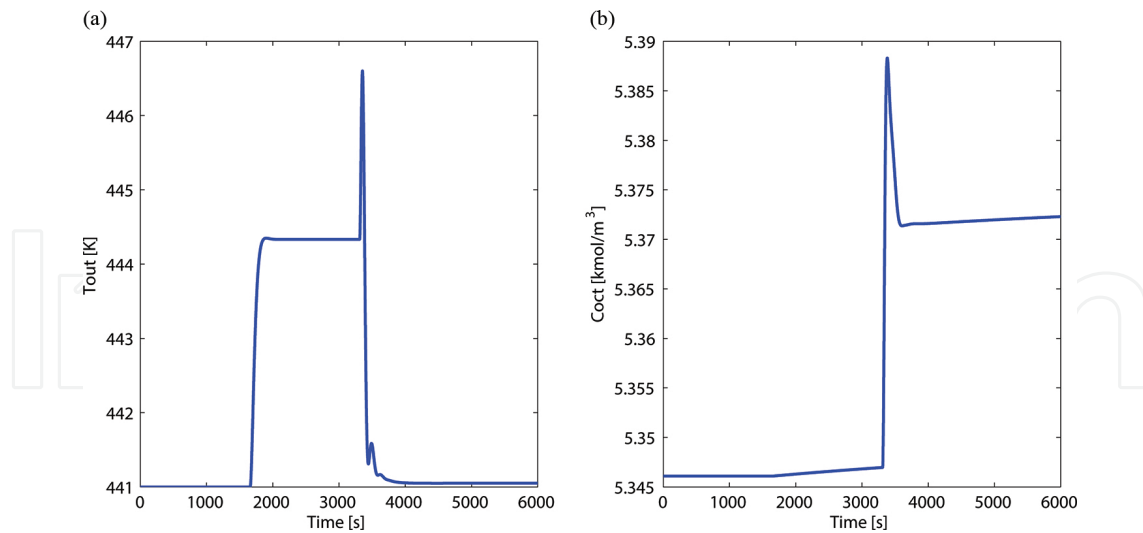


**Figure 11.** (a) Output temperature evolution and (b) 2 ethyl-hexanol concentration evolution considering a step variation in the 2 ethyl-hexanal input flow.

Based on the above results, the effectiveness of the proposed control is emphasized, presenting acceptable overshoot, response time and deviation values, but with opportunities for improvement. Thus, in the third scenario is considered an evolution for a period of 4 months and the catalyst activity degree is decreased up to 50%. **Figure 12** shows the temperature and 2 ethyl-hexanol concentration evolutions in this situation. It can be observed a steady error of 0.06% for the temperature and an error of 1% for the 2 ethyl-hexanol concentration.

The last simulation scenario is conceived in order to test the robustness of the designed control system for process parameter variations: gain variation and time constants variations (**Figure 13**).

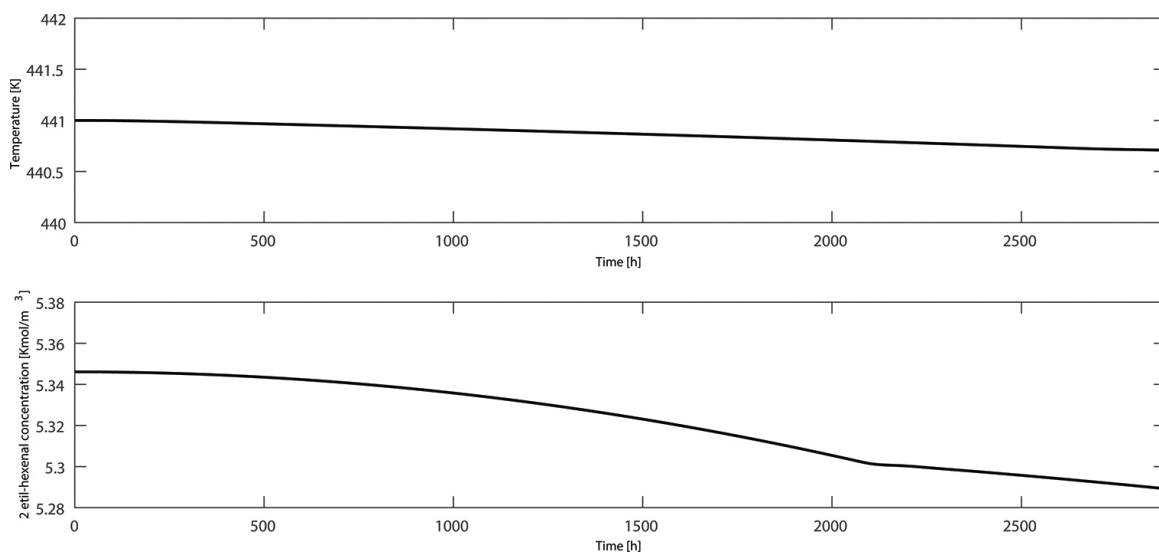


**Figure 12.** Catalyst deactivation: MIMO-SP PID controls.

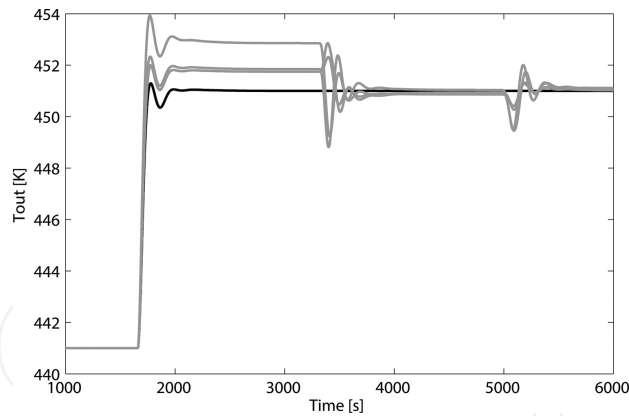


**Figure 13.** Output temperature evolution for reference step variation—nominal case vs. uncertain case (multivariable PID control).

A decrease in the control system performance can be observed, inferring reduced robustness, an aspect that may be improved by using advanced control strategies.

## 4. Design and implementation of advanced control strategies

### 4.1. Internal model control

The internal model control has emerged as an alternative to traditional feedback control algorithm feedback output as the simulation methods, mathematical modelling and model validation techniques developed [10]. This method provides a direct link between the process model and the controller structure. The IMC control structure is presented in **Figure 14** where  $p$  represents the transfer function describing the interconnections between process inputs  $u$  and outputs  $y$ ,  $p_d$  represents the transfer function that describes the effects of disturbance on the output,  $p_m$  is the mathematical model of the process and  $q$  is the transfer function of the IMC controller.

The model of the process is assumed to be equal to the process transfer function matrix presented before in Eq. (9) inferring the need of a Smith predictor structure:

$$\begin{bmatrix} T_{out} \\ C_{out} \end{bmatrix} = \begin{bmatrix} H_{f11m}(s) \cdot e^{-\sigma s} & H_{f12m}(s) \cdot e^{-\sigma s} \\ H_{f21m}(s) \cdot e^{-\sigma s} & H_{f22m}(s) \cdot e^{-\sigma s} \end{bmatrix} \begin{bmatrix} Q_{oct} \\ T_{in} \end{bmatrix}; \quad (12)$$

In order to ensure the process decoupling it is necessary to determine the pseudo-inverse matrix [11] of the steady state gain matrix:

$$H_m(0) = \begin{bmatrix} H_{f11m0} & H_{f12m0} \\ H_{f21m0} & H_{f22m0} \end{bmatrix} = \begin{bmatrix} -2.1 & 1 \\ -0.0049 & 0.011 \end{bmatrix} \quad (13)$$

$$H_m^\# = H_m(0)^H \cdot (H_m(0) \cdot H_m(0)^H)^{-1} = \begin{bmatrix} -0.6044 & 54.945 \\ -0.2692 & 115.384 \end{bmatrix} \quad (14)$$

The decoupled process is obtained as:  $H_D(s) = H_m(s)CH_m^\# = \begin{bmatrix} H_{f11d} & H_{f12d} \\ H_{f21d} & H_{f22d} \end{bmatrix}$ . Due to the static decoupling, steady-state matrix  $H_D(s=0)$  will be equal to the unit matrix, all the elements which are not on the first diagonal being equal to zero. Having the decoupled process the next step is to approximate the elements on the first diagonal of the matrix  $H_D(s)$  with simple transfer functions using identification methods:

$$H_{f11d}(s) = \frac{1 \cdot e^{-1650s}}{1055 \cdot s^2 + 55.85 \cdot s + 1}; H_{f22d}(s) = \frac{1 \cdot e^{-1650s}}{2204.1 \cdot s^2 + 69.64 \cdot s + 1} \quad (15)$$

The last step consists of the IMC controller design using:  $H_{RIMC}(s) = H_{f11d - inv}^*(s) \cdot f(s)$  where  $f(s)$  is the IMC filter:

$$f(s) = \frac{1}{(\lambda_i s + 1)^n} \quad (16)$$

where  $\lambda_i$  is the time constant of the filter associated to each output and  $n$  is chosen such as the final IMC controller is proper.

The obtained IMC controllers are:

$$H_{RIMC1}(s) = \frac{1055 \cdot s^2 + 55.85 \cdot s + 1}{400 \cdot s^2 + 40 \cdot s + 1}; H_{RIMC2}(s) = \frac{2204.1 \cdot s^2 + 69.64 \cdot s + 1}{100 \cdot s^2 + 20 \cdot s + 1} \quad (17)$$

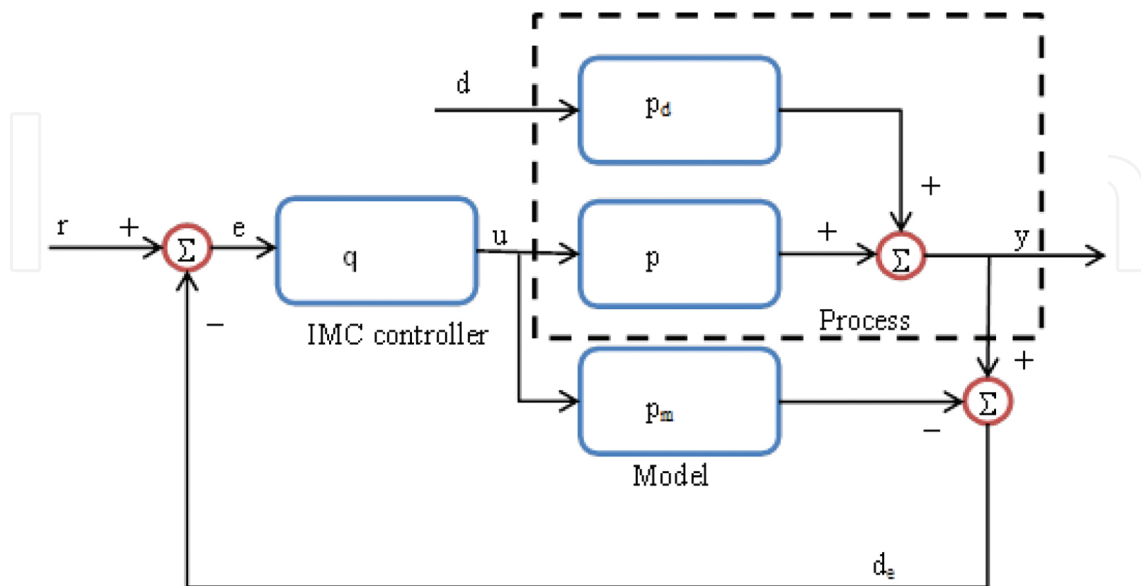
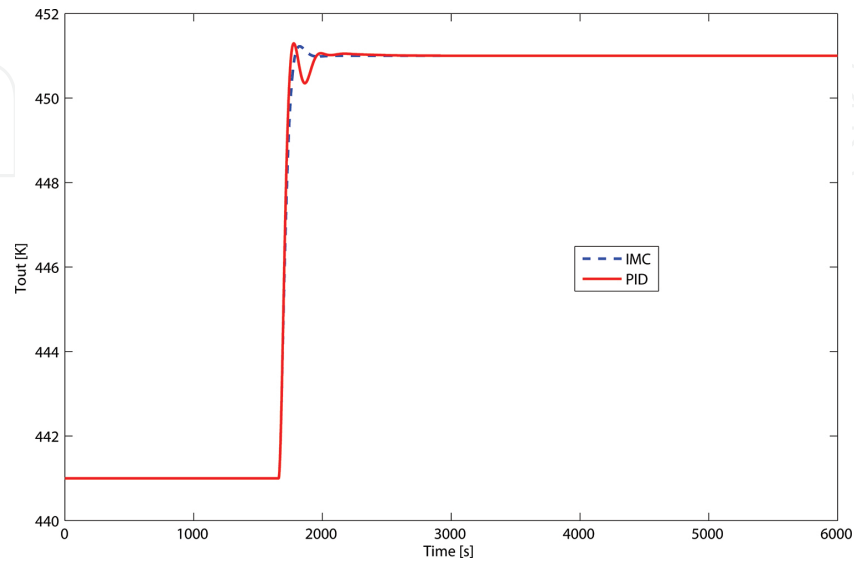


Figure 14. IMC control structure.



The IMC control system evaluation and testing are presented in comparison to the conventional multi-variable PID control strategy in order to conclude the results. To this end, the first test scenario consists in the set point tacking analysis. The simulation results are presented in **Figure 15**.



**Figure 15.** Output temperature evolution for reference step variation: PID vs. IMC.

The second simulation scenario is focused on the disturbance rejection analysis considering a  $0.25 \text{ [Kmol/m}^3\text{]}$  disturbance in the 2 ethyl-hexanal flow input flow (**Figure 16**).

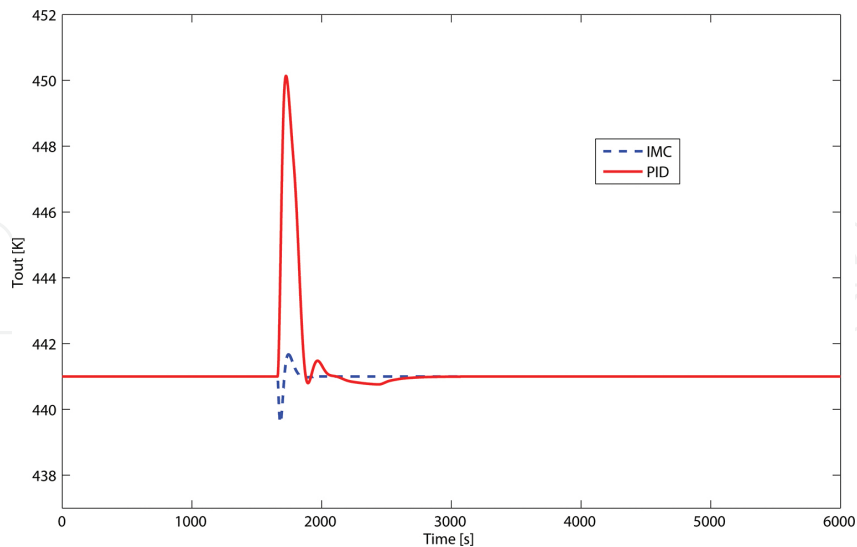


**Figure 16.** Output temperature evolution for a disturbance in the 2 ethyl-hexanal input flow: PID vs. IMC.

The third simulation scenario evaluates the IMC control system capability to counteract the effect of the catalyst deactivation (**Figure 17**).

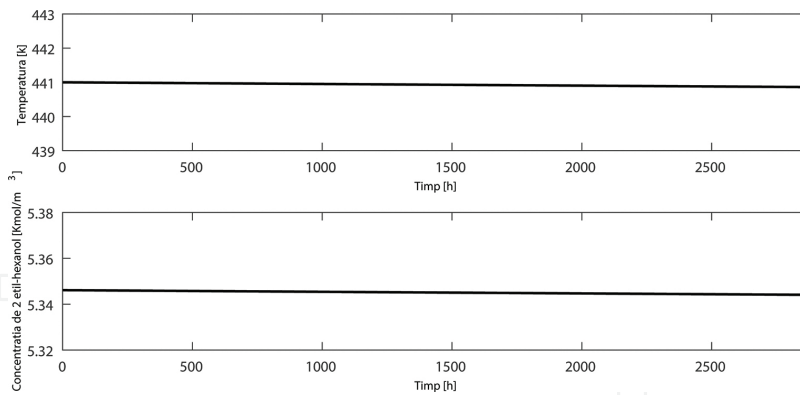


**Figure 17.** Catalyst deactivation: IMC control.

As in the previous case the last test scenario consists in the robustness evaluation of the IMC control system by considering the same variation of the process parameters (**Figure 18**).

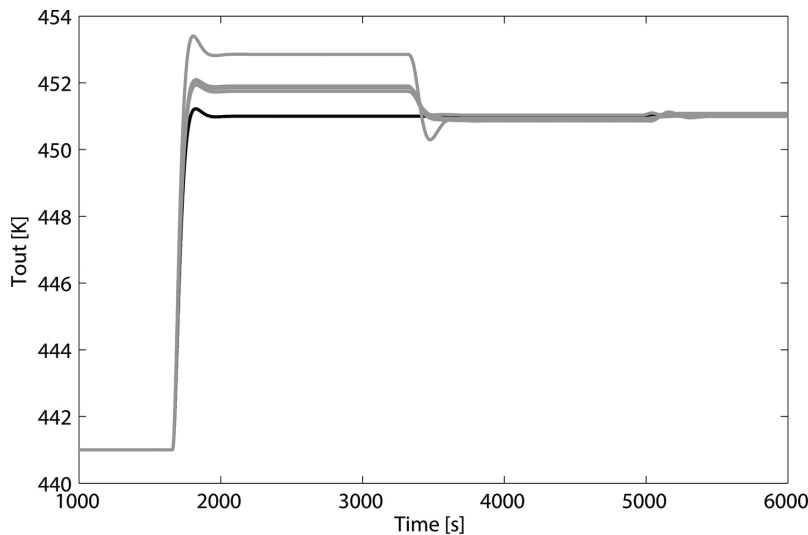


**Figure 18.** Output temperature evolution for reference step variation—nominal case vs. uncertain case (IMC control).

By analysing the comparative results between the MIMO SP-PID and SP-IMC control strategies it can be concluded that the SP-IMC control strategy outperforms the classical control. Another advantage is that it is easy to design and implement. However, even if the performances are clearly better the robustness to process parameter variations can be improved.

## 4.2. Robust control

Robust control can be defined as an attempt to control the uncertain systems (uncertainties). This approach accepts the idea of incomplete knowledge of the process, which has an uncertain dynamic and is influenced by disturbances insufficiently known. If, however, for these uncertainties can be established a mathematical norm, by using the robust control theory a robust, unique, able to meet certain performance specifications (hard or relaxed), controller

can be designed, respecting the uncertainty domain. Regardless of the method used to determine the mathematical model it is necessary to impose simplifying assumptions so that the obtained model is suitable for controller design. The differences between the real plant and the mathematical model represent modelling uncertainties or errors. Precisely from this view point the choice of robust control algorithms for the hydrogenation process 2-ethyl hexanal is justified. The robust controller design is a laborious task itself, but as the computational tools evolved the only difficult part left is the process parameter variation range determination. The same process operational model presented in Eq. (9) is used for multi-variable robust controller design based on  $H_{\infty}$  approach to ensure robust stability for both the nominal model and the entire class of systems that exist in a particular area of uncertainty around the nominal model. A Smith predictor MIMO structure is also necessary due to the large time delays presented by the hydrogenation process like in the previous sections.

$$\begin{bmatrix} T_{out} \\ C_{out} \end{bmatrix} = G_s \begin{bmatrix} Q_{oct} \\ T_{in} \end{bmatrix} + G_z \begin{bmatrix} Q_{enal} \\ P \end{bmatrix} \quad (18)$$

The first step was to determine the process state space representation:

$$\begin{aligned} \dot{X} &= A \cdot X + B \cdot U, X = \begin{bmatrix} T_{out} \\ C_{out} \end{bmatrix}; U = \begin{bmatrix} Q_{oct} \\ T_{in} \end{bmatrix} \\ Y &= C \cdot X + D \cdot U \end{aligned} \quad (19)$$

$$\begin{aligned} A &= \begin{bmatrix} a_{11} & a_{12} & 0 & 0 & 0 & 0 & 0 & 0 \\ a_{21} & 0 & 0 & 0 & 0 & 0 & 0 & 0 \\ 0 & 0 & a_{33} & a_{34} & 0 & 0 & 0 & 0 \\ 0 & 0 & a_{43} & 0 & 0 & 0 & 0 & 0 \\ 0 & 0 & 0 & 0 & a_{55} & a_{56} & 0 & 0 \\ 0 & 0 & 0 & 0 & a_{65} & 0 & 0 & 0 \\ 0 & 0 & 0 & 0 & 0 & 0 & a_{77} & a_{78} \\ 0 & 0 & 0 & 0 & 0 & 0 & a_{87} & 0 \end{bmatrix}; B = \begin{bmatrix} b_{11} & 0 \\ 0 & 0 \\ b_{31} & 0 \\ 0 & 0 \\ 0 & b_{52} \\ 0 & 0 \\ 0 & b_{72} \\ 0 & 0 \end{bmatrix} \\ C &= \begin{bmatrix} 0 & c_{12} & 0 & 0 & 0 & c_{16} & 0 & 0 \\ 0 & 0 & 0 & c_{24} & 0 & 0 & 0 & c_{28} \end{bmatrix}; D = \begin{bmatrix} 0 & 0 \\ 0 & 0 \end{bmatrix} \end{aligned} \quad (20)$$

The nominal values of the process parameters are:

$$\begin{aligned} \overline{a_{11}} &= -0.046, \overline{a_{12}} = -0.0225, \overline{a_{33}} = -0.0522, \overline{a_{34}} = -0.0279, \overline{a_{55}} = -0.0434, \\ \overline{a_{56}} &= -0.0207, \overline{a_{77}} = -0.0361, \overline{a_{78}} = -0.0176, \overline{a_{87}} = 0.0313, \overline{b_{31}} = 0.0156, \\ \overline{b_{72}} &= 0.0156, \overline{c_{12}} = -0.1890, \overline{c_{16}} = 0.1657, \overline{c_{24}} = -0.0087, \overline{c_{28}} = 0.0124 \end{aligned} \quad (21)$$

It is a well-known fact that, in real control systems, uncertainties are unavoidable and can negatively affect the stability and the performance of the whole control system. Usually, the uncertainties can be classified in two main categories: disturbance signals (input/output disturbance, sensor/actuator noise) and dynamic perturbations (difference between the actual dynamics of the process and the mathematical model) [12]. The dynamic perturbations are usually caused by inaccurate characteristic description, torn and worn effects and shifting operating points. They are also called 'parametric uncertainties' and are represented by certain process parameter variation over a certain value range. In a control system the dynamic

uncertainties can be represented in multiple ways. For this particular case the output multiplicative representation is considered showing the relative errors (between the actual system  $G_p(s)$  and the nominal model  $G_o(s)$ ) not only the absolute errors:  $G_p(s) = [I + \Delta(s)] G_o(s)$ . No matter what type of uncertainty representation is chosen, the actual, perturbed system can be represented like a standard upper linear fractional transform, where the uncertainties are lumped in a single block  $\Delta$ , a diagonal matrix corresponding to parameter variations (Figure 19).

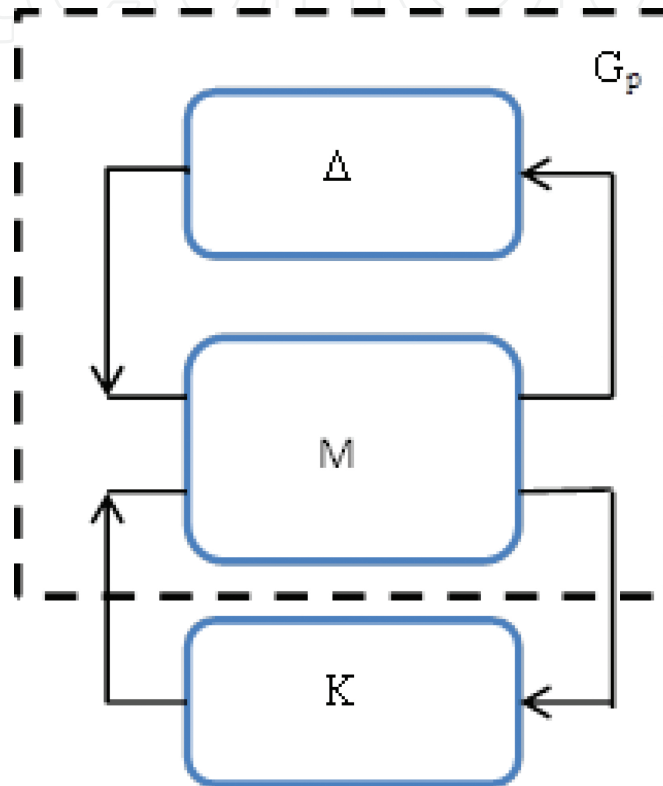


Figure 19. Generalized structure of the closed loop system.

The interconnection matrix for the considered multiplicative perturbation is:

$$M = \begin{bmatrix} 0 & G_o \\ I & G_o \end{bmatrix} \quad (22)$$

The uncertainty description is determined in an unconventional manner [13]. By using the experimental identification methods several second order models were determined using experimental data from different points of operation. In this way one can determine the interval for nominal model parameters variations.  $p_{11}$ ,  $p_{12}$ ,  $p_{33}$ ,  $p_{34}$ ,  $p_{55}$ ,  $p_{56}$ ,  $p_{77}$ ,  $p_{78}$ ,  $p_{87}$ ,  $p_{b31}$ ,  $p_{b72}$ ,  $p_{c12}$ ,  $p_{c16}$ ,  $p_{c24}$  and  $p_{c28}$  represent the computed possible, relative perturbation of the nominal process parameters. Each parameter  $a_{ij}$ ,  $b_{ij}$  and  $c_{ij}$  ( $i, j = 1,8$ ) may be represented as a linear fractional transformation (LFT) considering multiplicative uncertainties.

The next step is to determine the process mathematical model that takes into account also the model parameter uncertainties,  $G_{mds}$  having the following form [12]:

$$G_{mds} = \left[ \begin{array}{c|cc} \underline{A} & \underline{B1} & \underline{B2} \\ \hline \underline{C1} & \underline{D11} & \underline{D12} \\ \underline{C2} & \underline{D21} & \underline{D22} \end{array} \right] \tag{23}$$

$$A = \begin{bmatrix} a11 & a12 & 0 & 0 & 0 & 0 & 0 & 0 & 0 \\ a21 & 0 & 0 & 0 & 0 & 0 & 0 & 0 & 0 \\ 0 & 0 & a33 & a34 & 0 & 0 & 0 & 0 & 0 \\ 0 & 0 & a43 & 0 & 0 & 0 & 0 & 0 & 0 \\ 0 & 0 & 0 & 0 & a55 & a56 & 0 & 0 & 0 \\ 0 & 0 & 0 & 0 & a65 & 0 & 0 & 0 & 0 \\ 0 & 0 & 0 & 0 & 0 & a77 & a78 & 0 & 0 \\ 0 & 0 & 0 & 0 & 0 & 0 & a87 & 0 & 0 \end{bmatrix}; B2 = \begin{bmatrix} b11 & 0 \\ 0 & 0 \\ b31 & 0 \\ 0 & 0 \\ 0 & b52 \\ 0 & 0 \\ 0 & b72 \\ 0 & 0 \end{bmatrix}; C1 = \begin{bmatrix} a11 & a12 & 0 & 0 & 0 & 0 & 0 & 0 & 0 \\ a21 & 0 & 0 & 0 & 0 & 0 & 0 & 0 & 0 \\ 0 & 0 & a33 & a34 & 0 & 0 & 0 & 0 & 0 \\ 0 & 0 & a43 & 0 & 0 & 0 & 0 & 0 & 0 \\ 0 & 0 & 0 & 0 & a55 & a56 & 0 & 0 & 0 \\ 0 & 0 & 0 & 0 & a65 & 0 & 0 & 0 & 0 \\ 0 & 0 & 0 & 0 & 0 & a77 & a78 & 0 & 0 \\ 0 & 0 & 0 & 0 & 0 & 0 & a87 & 0 & 0 \\ 0 & 0 & 0 & 0 & 0 & 0 & 0 & 0 & 0 \\ 0 & 0 & c12 & 0 & 0 & 0 & 0 & 0 & 0 \\ 0 & 0 & 0 & 0 & c16 & 0 & 0 & 0 & 0 \\ 0 & 0 & 0 & c24 & 0 & 0 & 0 & 0 & 0 \\ 0 & 0 & 0 & 0 & 0 & 0 & c28 & 0 & 0 \end{bmatrix}; D12 = \begin{bmatrix} 0 & 0 \\ 0 & 0 \\ 0 & 0 \\ 0 & 0 \\ 0 & 0 \\ 0 & 0 \\ 0 & 0 \\ 0 & 0 \\ 0 & 0 \\ b31 & 0 \\ 0 & b72 \\ 0 & 0 \\ 0 & 0 \\ 0 & 0 \\ 0 & 0 \end{bmatrix} \tag{24}$$

$$B1 = \begin{bmatrix} p11 & p12 & 0 & 0 & 0 & 0 & 0 & 0 & 0 & 0 & 0 & 0 & 0 & 0 & 0 \\ 0 & 0 & 0 & 0 & 0 & 0 & 0 & 0 & 0 & 0 & 0 & 0 & 0 & 0 & 0 \\ 0 & 0 & p33 & p34 & 0 & 0 & 0 & 0 & pb31 & 0 & 0 & 0 & 0 & 0 & 0 \\ 0 & 0 & 0 & 0 & 0 & 0 & 0 & 0 & 0 & 0 & 0 & 0 & 0 & 0 & 0 \\ 0 & 0 & 0 & 0 & p55 & p56 & 0 & 0 & 0 & 0 & 0 & 0 & 0 & 0 & 0 \\ 0 & 0 & 0 & 0 & 0 & 0 & 0 & 0 & 0 & 0 & 0 & 0 & 0 & 0 & 0 \\ 0 & 0 & 0 & 0 & 0 & 0 & p77 & p78 & 0 & 0 & pb72 & 0 & 0 & 0 & 0 \\ 0 & 0 & 0 & 0 & 0 & 0 & 0 & 0 & 0 & 0 & pb72 & 0 & 0 & 0 & 0 \\ 0 & 0 & 0 & 0 & 0 & 0 & 0 & 0 & 0 & 0 & 0 & 0 & 0 & 0 & 0 \end{bmatrix}; C2 = \begin{bmatrix} 0 & c12 & 0 & 0 & 0 & c16 & 0 & 0 \\ 0 & 0 & 0 & c24 & 0 & 0 & 0 & c28 \end{bmatrix}; D22 = \begin{bmatrix} 0 & 0 \\ 0 & 0 \end{bmatrix}$$

$$D21 = \begin{bmatrix} 0 & 0 & 0 & 0 & 0 & 0 & 0 & 0 & 0 & 0 & pc12 & pc16 & 0 & 0 \\ 0 & 0 & 0 & 0 & 0 & 0 & 0 & 0 & 0 & 0 & pc24 & pc28 \end{bmatrix}; D11 = \text{zeros}(15,15)$$

The block diagram of the closed loop system in Smith predictor structure including the robust multi-variable controller and the uncertainties bloc is presented in **Figure 20**.

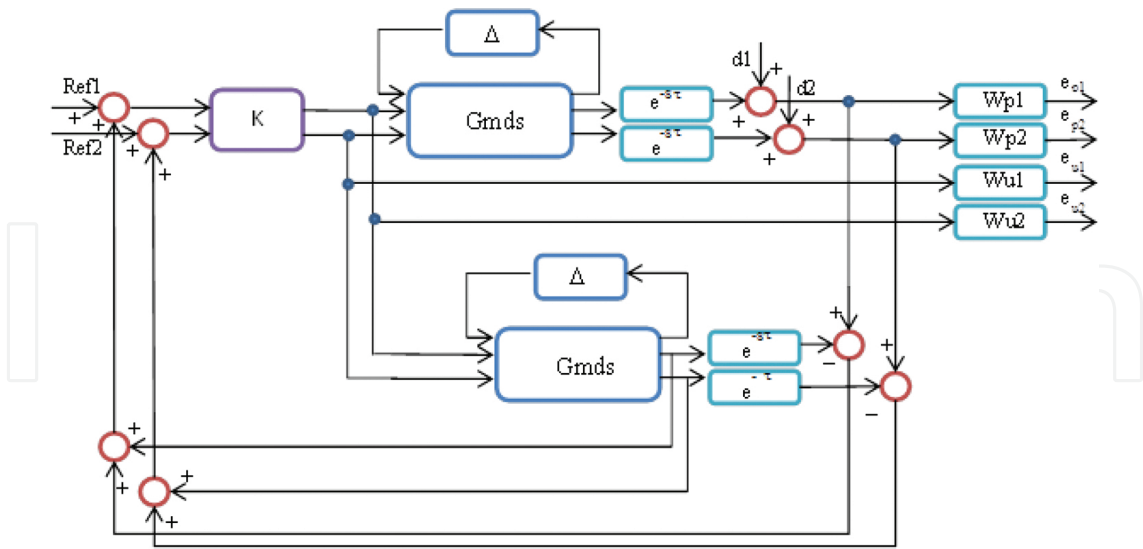


**Figure 20.** The MIMO-SP closed loop control structure using robust controller.

As it can be observed  $G_{mds}$  is nominal model of the process,  $d1, d2$  represent the disturbances,  $\Delta$  is the matrix uncertainties,  $Wu1, Wu2$  and  $WP1, WP2$  are weighting functions which reflect the relative significance of performance requirements. For good mitigation of disturbances and

to ensure a certain response time and overshoot Wu1, Wu2 and WP1, WP2 have the following form:

$$Wp1(s) = 0.9 \frac{s^2+2s+5}{s^2+1.1s+0.02}; Wp2(s) = 0.1 \frac{s+3}{s+0.1}; Wu1 = 10^{-5}; Wu2 = 10^{-5} \quad (25)$$

It should be noted that choosing the suitable weighting functions is a crucial step in the synthesis of robust controller and usually requires several attempts. By applying the presented method, using MATLAB/SIMULINK environment – *hinfsyn* function, the following robust  $H_\infty$  controller was determined:

$$A_K = \begin{bmatrix} -29.50 & -1.48e4 & 8.65 & 159.78 & 25.83 & 1.29e4 & -12.5 & -227.8 & -1.62e5 & -1e535 & -8.39e3 \\ & 0.313 & 0 & 0 & 0 & 0 & 0 & 0 & 0 & 0 & 0 \\ -1.83 & -923.8 & 0.48 & 9.94 & 1.61 & 809.99 & -0.78 & -14.21 & -1.016e4 & -8.43e3 & -523.69 \\ & 0 & 0 & 0.0313 & 0 & 0 & 0 & 0 & 0 & 0 & 0 \\ 5.45 & 3.22e3 & 9.73 & 178.2 & -4.82 & -2.8271e3 & -14.06 & -254.1 & 3.56e4 & 2.95e4 & -9.24e3 \\ & 0 & 0 & 0 & 0.0313 & 0 & 0 & 0 & 0 & 0 & 0 \\ 0.68 & 402.42 & 1.21 & 22.24 & -0.59 & -352.81 & -1.79 & -31.73 & 4.45e3 & 3.69e3 & -1.15e3 \\ & 0 & 0 & 0 & 0 & 0.0313 & 0 & 0 & 0 & 0 & 0 \\ & 0 & 0 & 0 & 0 & 0 & 0.0313 & 0 & 0 & 0 & 0 \\ & 0 & 0 & 0 & 0 & 5.55e-17 & 0 & 0 & -0.0175 & -0.0317 & 0 \\ & 0 & -5.55e-17 & 0 & 0 & 5.55e-17 & 0 & 0 & 0.0317 & -1.08 & 0 \\ & 0 & 0 & 0 & -8.67e-19 & 0 & 0 & 0 & 0 & 0 & -0.1 \end{bmatrix}; B_K = \begin{bmatrix} 0 & 0 \\ 0 & 0 \\ 0 & 0 \\ 0 & 0 \\ 0 & 0 \\ 0 & 0 \\ 0 & 0 \\ 0.0255 & 0 \\ -0.0288 & 0 \\ 0 & -0.0069 \end{bmatrix} \quad (26)$$

$$C_k = \begin{bmatrix} -9.2e3 & -4.6e6 & 2.7e3 & 4.9e4 & 8.07e3 & 4.05e6 & -3.9e3 & -7.11e4 & -5.08e7 & -4.2e7 & -2.6e6 \\ 3.4e3 & 2.01e6 & 6.8e3 & 3.11e5 & -2.9e3 & -1.76e6 & -8.79e3 & -1.58e5 & 2.22e7 & 1.84e7 & -5.7e6 \end{bmatrix}; D_K = \begin{bmatrix} 0 & 0 \\ 0 & 0 \end{bmatrix}$$

Like for the previous control strategies the first simulation test scenario consists of closed loop simulation evaluation under nominal parameter values. The same simulation scenario was performed for the whole class of systems in the uncertainty domain for a reference step variation for the output temperature. The simulation results show good performances of the developed control structure even considering the process parameter uncertainty domain (Figure 21).

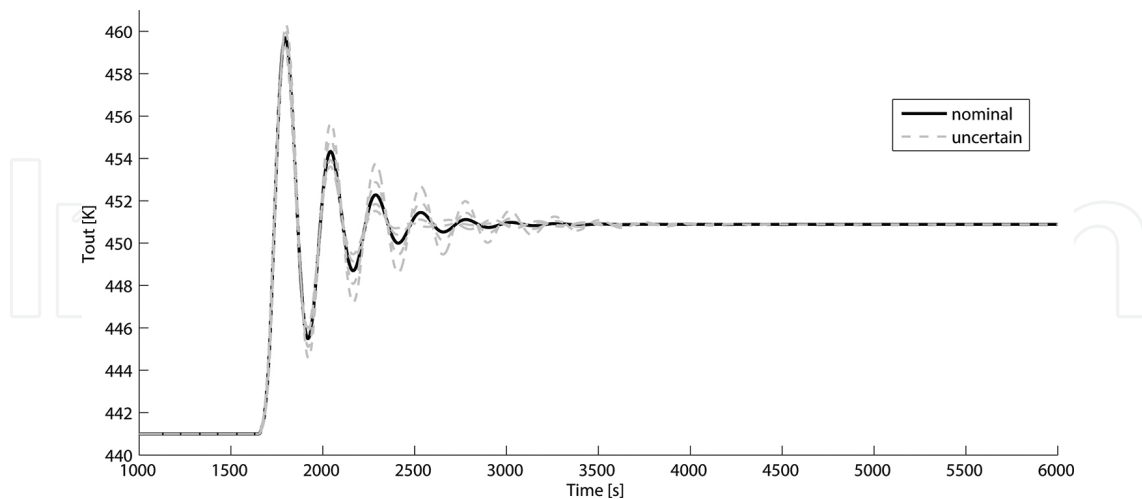
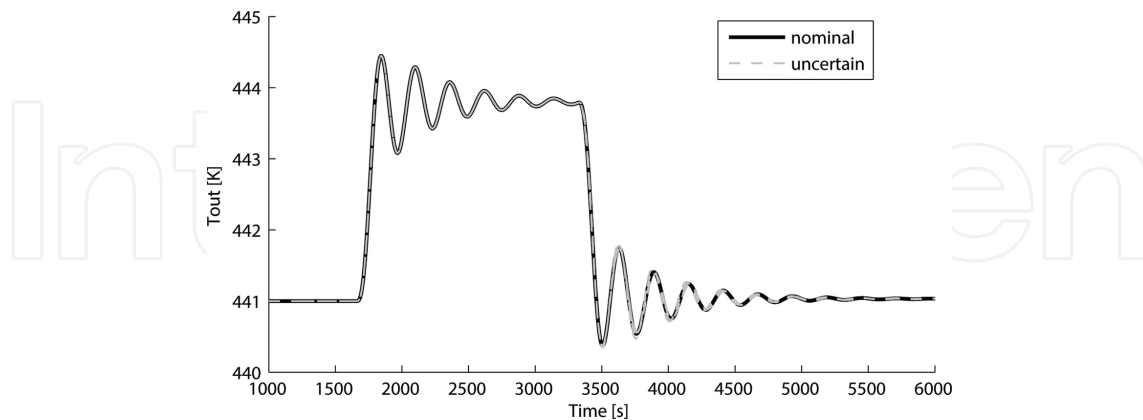


Figure 21. Output temperature evolution—robust controller: nominal vs. uncertain considering a reference step variation.

The second simulation scenario will evaluate the capability to reject the disturbance effect and also to test at the same time the robustness of the system. To this end, a step variation of the 2

ethyl-hexanal input flow is considered along with the process parameter variations. Good performances are reached even in the case of the uncertain plants (**Figure 22**).



**Figure 22.** Output temperature evolution—robust controller: nominal vs. uncertain considering a reference step variation of the 2 ethyl-hexanal input flow.

Another performance that needs to be evaluated is the ability to counter act the catalyst deactivation effect (**Figure 23**).

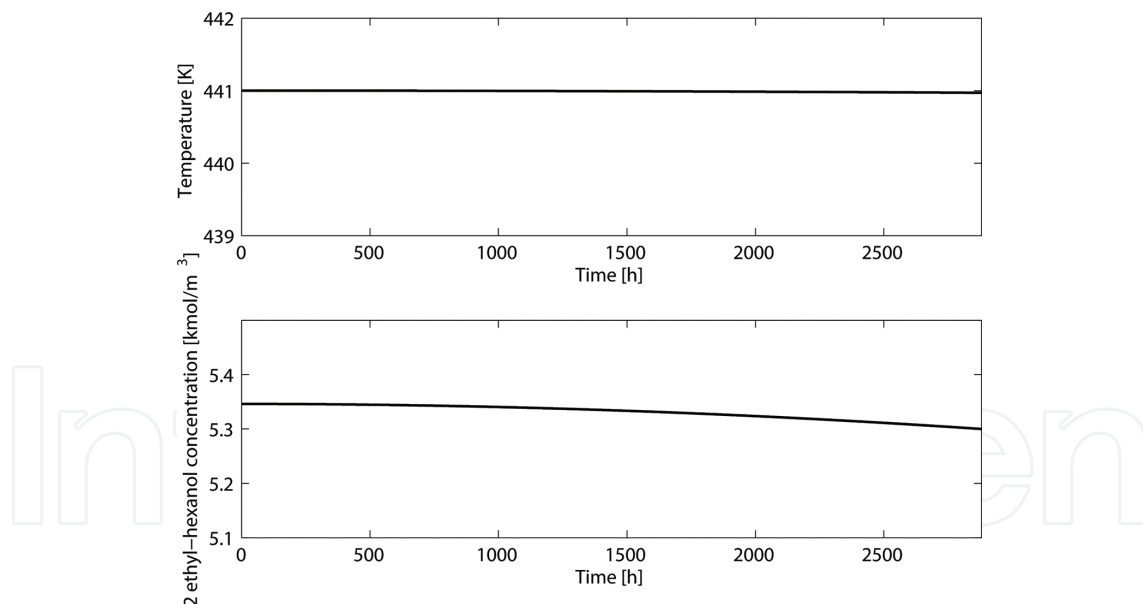


**Figure 23.** Catalyst deactivation: robust controller.

By analysing all the results obtained in the previous figures it can be concluded that even considering the catalyst deactivation steady-state errors of 0.006% and 0.18% are achieved for the output temperature and 2 ethyl-hexanol concentration, which are clearly within acceptable limits making the robust control strategy the most suitable for 2 ethyl-hexanal hydrogenation process control.

## 5. Conclusions

The developed model of the hydrogenation process, presented in this chapter, is able to represent the dynamic behaviour of the reactor during operation. Real plant data was used for mathematical model validation. From the dynamic point of view, the system behaves as an element with a large time constant and a large time delay. Hydrogenation multiphase catalytic reactors have complex behaviour and from this point of view, the use of advanced control strategies together with online optimization techniques appears to be a suitable procedure to deal with the problem of operating at high level of performance and safety.

A possibility to describe the processes which occur inside the reactor by a linear nominal transfer matrix and uncertainty description is detailed. A practical method for obtaining the uncertainty description is also presented. Three control strategies are proposed, developed, implemented and tested.

Finally, a comparison between the advantages and disadvantages of the proposed control solutions is performed.

## Acknowledgements

This work was supported by a grant of the Romanian National Authority for Scientific Research and Innovation, CNCS- UEFISCDI, project number 155/2012 PN-II-PT-PCCA.

## Nomenclature

Symbol	Description
$C_i$	molar concentration (kmol/m <sup>3</sup> ) of component $i$ : enal (2 ethyl-hexanal), anal (2 ethyl-hexanal), oct (2 ethyl-hexanol)
$C_H^L$	concentration of hydrogen in liquid phase
$C_H^G$	concentration of hydrogen in gaseous phase
$Q_i$	volumetric flow rate (m <sup>3</sup> /s) of component in phase $i$ : L(liquid), G(gaseous)
$T$	temperature (K)
$c_p$	specific heat capacity (kJ/kg K)
$a_v$	specific gas-liquid contact area (m <sup>-1</sup> )
$z$	axial reactor coordinate
$S$	cross-sectional area
$r_i$	rate of surface reaction $i$ : 1, 2
$K_i$	adsorption equilibrium constant, component $i$ (m <sup>3</sup> /mol)



Symbol	Description
$k_j$	rate constant of surface reaction $j$ (mol/s kg)
$\rho_{sol}$	solution density (kg/m <sup>3</sup> )
$N_{HG}$	the flux of hydrogen transferred from gaseous phase to liquid phase [5, 7] $N_{HG} = K_{L,H}(C_H^* - C_{H,L})$ $\frac{1}{K_{L,H}} = \frac{1}{H_H C k_G} + \frac{1}{k_{L,H}}$ $C_H^* = p_H / H_H$
$v_{ph}$	the transferred hydrogen flow through the liquid film, adjacent to the catalyst pellet, on to its' surface [5, 7] $v_{ph} = \frac{M_{L,H}}{2K_H} \left[ \left( \frac{w \cdot k_1 \cdot \eta_i}{M_{L,H}} + \frac{K_H \cdot p_H}{H_H} + 1 \right) - \sqrt{\left( \frac{w \cdot k_1 \cdot \eta_i}{M_{L,H}} + \frac{K_H \cdot p_H}{H_H} + 1 \right)^2 - 4 \frac{K_H}{M_{L,H}} \cdot \frac{w \cdot k_1 \cdot \eta_i \cdot p_H}{H_H}} \right]$ $\frac{1}{M_{L,H}} = \frac{1}{a_v \cdot K_{L,H}} + \frac{1}{a_S \cdot k_{S,H}}$
$\Delta_r H_i$	the reaction heat of reaction $i:1, 2$ (kJ/kmol)
$p_H$	partial pressure of hydrogen in the convective zone of the gas phase [atm]
$H_H$	Henry's law constant (atm m <sup>3</sup> /Kmol)

## Author details

Roxana Rusu-Both

Address all correspondence to: roxana.both@aut.utcluj.ro

Technical University of Cluj-Napoca, Cluj-Napoca, Romania

## References

- [1] ICIS. [Internet]. Available from: www.icis.com [Accessed: 2016-03-15].
- [2] Smelder G. Kinetic analysis of the liquid phase hydrogenation of 2-ethyl-hexenal in the presence of supported Ni,Pd and Ni-S catalyst. The Canadian Journal of Chemical Engineering. 1989;67:51–61. DOI: 10.1002/cjce.5450670109
- [3] Olah GA, Molnar A. Hydrocarbon Chemistry. 2nd ed. New York: John Wiley & Sons; 2003. 871 p. DOI: 10.1002/0471433489

- [4] Bâldea I. Kinetics and Reaction Mechanisms (in Romania). Cluj-Napoca: University Publishing House Cluj; 2002. ISBN 973-610-130-4
- [5] Bozga G, Muntean O. Chemical Reactors (in Romanian). Bucuresti: Technical Publishing House; 2001. ISBN 9733115789
- [6] Popovici C.I. Numerical Analysis with Matlab (in Romanian). Iasi: Venus Publishing House; 2007. 408 p. ISBN 978-973-756-043-8
- [7] Both R, Cormos AM, Agachi PS, Festilă C. Dynamic modeling and validation of the 2 ethyl-hexenal hydrogenation process. *Computer & Chemical Engineering Journal*. 2013;52:100–111. DOI: 10.1016/j.compchemeng.2012.11.012
- [8] Melo DNC, Costa CBB, Toledo ECV, Santos MM, Maciel MRW, Filho RM. Evaluation of control algorithms for three phase hydrogenation catalytic reactors. *Chemical Engineering Journal*. 2008;141:250–263. DOI: 10.1016/j.cej.2007.12.026
- [9] Wang QG, He Z, Cai W-J, Hang CC. PID Control for Multivariable Processes. Berlin, Heidelberg: Springer-Verlag; 2008. 266 p. DOI: 10.1007/978-3-540-78482-1
- [10] Agachi PS, Nagy ZK, Cristea VM, Lucaci A. Model Based Control. Weinheim, Germany: Wiley-VCH Verlag GmbH & Co. KGaA; 2006. DOI: 10.1002/9783527609475
- [11] Skogestad S, Postlethwaite I. Multivariable Feedback Control: Analysis and Design. New York: John Wiley & Sons; 2005. 590 p. ISBN 978-0-470-01167-6
- [12] Gu DW, Petkov PH, Konstantinov MM. Robust Control Design with MATLAB. 1st ed. London, Springer-Verlag; 2005. 389 p. ISBN-10: 1-85233-983-7
- [13] Both R, Dulf EH, Festilă C, Agachi PS. Robust control of a catalytic 2 ethyl-hexenal hydrogenation reactor. *Journal of Chemical Engineering Science*. 2012;74:300–309. DOI: 10.1016/j.ces.2012.02.033

IntechOpen

